ELSEVIER

0141-1187(95)00014-3

Applied Ocean Research 17 (1995) 185–204

0141-1187/95/$09.50

Chaotic roll motion and capsize of ships under periodic excitation with random noise

Huan Lin & Solomon C. S. Yim*

Ocean Engineering Program, Department of Civil Engineering, Oregon State University, Corvallis, Oregon 97331-2303, USA

(Received 11 February 1994; accepted 25 April 1994)

A stochastic analysis procedure is developed to examine the properties of chaotic roll motion and the capsize of ships subjected to periodic excitation with a random noise disturbance. To take into account the presence of randomness in the excitation and the response, a generalized Melnikov method is developed to provide an upper bound on the domain of the potential chaotic roll motion. The associated Fokker–Planck equation governing the evolution of the probability density function (PDF) of the roll motion is derived and numerically solved by the path integral solution procedure to obtain joint probability density functions (JPDFs) in state space. A chaotic response can be found in two regions (near the homoclinic and heteroclinic orbits). The global behavior of the roll motion can be depicted by the JPDF. It is found that the presence of noise enlarges the boundary of the chaotic domains and bridges coexisting attracting basins in the local regimes. The attracting domain of capsize is of the greatest strength. The probability of capsize is considered in this paper as an extreme excursion problem with the time-averaged PDF as an invariant measure. With this measure, the heteroclinic region is identified as an 'unsafe' regime. Numerical results indicate that, under the presence of noise, all roll motion trajectories of a ship that visit the regime near the heteroclinic orbit will eventually lead to capsize.

1 INTRODUCTION

Ship dynamics often contain complicated non-linear physical behavior. In particular, the associated stability of roll motion is of great practical importance. Existing stability criteria are expressed in terms of minimum values of certain key features of the righting arm or the *GZ* curve. For certain classes of ship, static stability standards based on statistical and other analyses of intact static conditions are sufficient for design purposes, and can give a qualitative understanding of the stability behavior for the naval architect.[1] Although the *GZ* curve is found to be an important ship characteristic in assuring safety,[2] other ship properties are also significant. These include hydrodynamic and viscous roll damping, as affected by the wave exciting force, initial conditions, and the presence of water on deck. The dynamics of a ship rolling in a regular seaway can be highly non-linear. Harmonic, subharmonic or even chaotic motions may occur.

*Currently visiting the Naval Architecture and Offshore Engineering Department, University of California, Berkeley, California 94720, USA.

In recent works, the non-linear mechanism of ship roll motion has been depicted by applying global stability analyses. One approach [1,3–8] is to generate invariant manifolds and simulate roll responses corresponding to fine grids of initial conditions. Detailed pictures of the basin boundaries between bounded and escaping (divergent and hence capsizing) motions are constructed. The results illustrate the manner in which systems that are inherently safe when unforced become unsafe as periodic excitation is applied. Another approach[2] is to generate the invariant manifolds and employ the concept of lobe dynamics to demonstrate the mechanism of 'unexpected capsize'. In practice, long trains of pure regular waves do not exist—the presence of discernable environmental disturbances is inevitable. The perturbed waveforms may be modeled as regular waves with random noise as the external disturbance. Thus, the ship's roll motion under perturbed regular waves can be considered as a noise-disturbed non-linear system, which has been of interest to researchers in various science and engineering fields in recent years.

Bulsara *et al.*[9] introduced the generalized version of the Melnikov function for providing the criterion for chaotic response in the presence of noise. They

embedded the noise in the Hamiltonian system to form noisy homoclinic orbits, and inferred that, on average, the threshold for chaotic response is elevated by the presence of noise. A parallel investigation of the generalized Melnikov function was conducted by Frey and Simiu.[10] They approximated ideal white noise by adopting Shinozuka's band-limited noise representation, which is considered as a perturbation to a homoclinic orbit. By applying the concept of average flux, they concluded that chaotic motion is not suppressed by the presence of weak noise.

Probability density functions (PDFs) have also been utilized to depict the stochastic properties of noisy non-linear systems. Kapitaniak[11] solved the associated Fokker–Planck equation of a dynamic system with noise and illustrated that the noisy chaotic response is characterized by a nonstationary multi-maxima marginal PDF. Bulsara *et al.*[12] investigated the noise effect on the behavior of non-linear systems through the Lyapunov exponent and the PDF. A smoothing effect of noise on the PDF depicting the chaotic attractor and noise-induced chaotic motions was observed through numerical simulations. Kunert and Pfeiffer[13] employed a finite-difference procedure to solve the Fokker–Planck equation. The resulting steady-state joint probability density function (JPDF) shows the imprint of the corresponding chaotic attractor on the Poincaré section.

The invariant properties of noisy chaotic motions have also been examined. Kifer[14] proved the existence of invariant measures of attractors under noisy disturbances. Jung and Hänggi[15] proposed the time-averaged PDF as an invariant measure for deterministic and noisy chaos.

The objective of this investigation is to gain a better understanding of the non-linear behavior of ship roll motion and capsize under perturbed regular waves, with the disturbance approximated by white noise. The system model considered approximates the roll motion of a ship with water on deck. This model reveals two distinct (i.e. homoclinic and heteroclinic) dynamic regions.[2] The criterion for noisy chaotic roll motion and a global description of the system's behavior for each region will be derived. The noise effects on the non-linear roll response and the probability of capsize will be investigated.

The criterion for chaotic roll motion under noisy regular waves will be derived through the generalized Melnikov function which is derived in this study by expanding the analysis in Frey and Simiu.[10] By taking one step further, a mean-square representation of the Melnikov criterion will be developed to provide an upper bound to the domain of possible chaotic response in parameter space. However, in this study, ideal white noise, rather than Shinozuka's band-limited noise, will be utilized.

The global behavior of the noisy non-linear roll motion can be described by the evolution of the PDF characterized by the Fokker–Planck equation. A path integral solution procedure will be employed to compute the transient and steady-state JPDFs. Local existing attractors will be depicted by the steady-state PDF. The noise effect on a single chaotic attractor and coexisting periodic and chaotic attractors will be examined. Finally, the relationship between chaotic roll motion and capsize will be illustrated stochastically through the JPDFs. The probability of capsize will be considered as an extreme excursion problem and investigated with the time-averaged PDF as an invariant measure.

This paper represents a first attempt to study the qualitative behavior of the chaotic motion and capsize of ships in probability space. The goal is to provide a foundation for stochastic analysis of highly non-linear ocean systems. To keep the analysis manageable and for clarity of presentation, pure roll motion is assumed. More realistic systems with coupled roll, heave and sway motions and potential applications of the probability-space approach will be examined in future studies.

2 THE SYSTEM UNDER CONSIDERATION

The system considered in this study describes a single degree-of-freedom ship roll motion under periodic (sinusoidal) waves with additive Gaussian white noise. Assuming a beam sea condition and that the roll motion is uncoupled from other degrees of freedom, the governing equation can be expressed as follows[2]

$$[I_{44} + A_{44}(\omega)]\ddot{\phi} + B_{44}(\omega)\dot{\phi} + B_{44q}(\omega)\dot{\phi}|\dot{\phi}| + \Delta G Z_m(\phi) = F_{sea}(\omega)\cos(\omega t + \epsilon_4) + \xi(t) \quad (1)$$

where ϕ is the roll angle, I_{44} is the moment of inertia (in air) of the ship about the roll axis, A_{44} is the hydrodynamic added mass coefficient, B_{44} is the linear roll damping coefficient, B_{44q} is the quadratic drag coefficient, Δ is the ship's weight, and $GZ_m(\phi)$ is a polynomial approximation to the non-linear roll-restoring moment-arm. F_{sea}, ω and ϵ_4 are the amplitude, frequency and phase shift of the external wave exciting force, respectively. $\xi(t)$ is an ideal, zero-mean, delta-correlated Gaussian white noise, i.e.

$$\langle \xi(t) \rangle = 0$$

$$\langle \xi(t')\xi(t) \rangle = \nu\delta(t' - t) \quad (2)$$

where $\langle \ldots \rangle$ represents the ensemble average, $\delta(\ldots)$ is the Dirac delta function, and ν is the noise intensity. This additive Gaussian white noise approximates the disturbance in a sinusoidal external periodic force. By including the effect of water on deck, the roll motion is characterized by two distinct dynamics in different regions—homoclinic and heteroclinic.[2] Assuming frequency-independent coefficients, dividing eqn (1) by the inertia coefficient (mass plus added mass), taking a two-

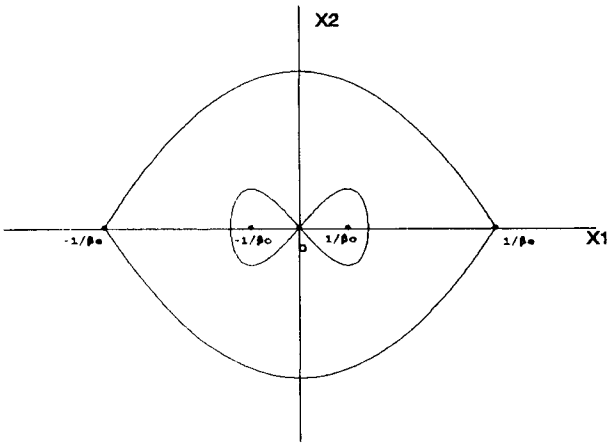

Fig. 1. Homoclinic (inside) and heteroclinic orbits in unperturbed rolling motion.

term polynomial approximation of the $GZ_m(\phi)$ curve, and rescaling time, the non-dimensionalized versions of the homoclinic and heteroclinic dynamics are obtained, respectively, as follows:

$$\ddot{x} + \alpha\dot{x} + \alpha_q\dot{x}|\dot{x}| - x + \beta_0^2x^3 = A\cos(\Omega\tau + \Psi) + \eta(\tau) \tag{3}$$

and

$$\ddot{x} + \alpha\dot{x} + \alpha_q\dot{x}|\dot{x}| + x - \beta_e^2x^3 = A\cos(\Omega\tau + \Psi) + \eta(\tau) \tag{4}$$

where

$$\langle\eta(\tau)\rangle = 0$$

$$\langle\eta(\tau')\eta(\tau)\rangle = \kappa\delta(\tau' - \tau) \tag{5}$$

and κ represents the noise intensity.

The unperturbed systems can be obtained by introducing two state variables:

$$X = \begin{Bmatrix} x \\ \dot{x} \end{Bmatrix} = \begin{Bmatrix} x_1 \\ x_2 \end{Bmatrix} \tag{6}$$

then

$$\dot{X} = f_1(X) = \begin{Bmatrix} \dfrac{\partial H_1(x_1, x_2)}{\partial x_2} \\ \dfrac{\partial H_1(x_1, x_2)}{\partial x_1} \end{Bmatrix} = \begin{Bmatrix} x_2 \\ x_1 - \beta_0^2x_1^3 \end{Bmatrix} \tag{7}$$

and

$$\dot{X} = f_2(X) = \begin{Bmatrix} \dfrac{\partial H_2(x_1, x_2)}{\partial x_2} \\ \dfrac{-\partial H_2(x_1, x_2)}{\partial x_1} \end{Bmatrix} = \begin{Bmatrix} x_2 \\ -x_1 + \beta_e^2x_1^3 \end{Bmatrix} \tag{8}$$

where the state variables x_1 and x_2 represent the roll angle and velocity, respectively, and $H_{1,2}(x_1, x_2)$ are the Hamiltonians.

There are three fixed points for eqn (7): at (0, 0) and $(\pm 1\beta_0, 0)$, which represent an unstable upright equilibrium position (local saddle) and the positive and negative loll angles (two centers), respectively. Moreover, three fixed points for eqn (8), at (0, 0) and $(\pm 1/\beta_e, 0)$, represent a global center, and positive and negative angles of vanishing stability (saddles), respectively. The associated phase plane is shown in Fig. 1, in which a pair of homoclinic orbits (inside, small amplitude roll motions) and a pair of heteroclinic orbits (outside, relatively large amplitude roll motions) are depicted. Equations (3) and (4) govern the dynamics of the roll motion in the local homoclinic and heteroclinic regions, respectively. Accordingly, the ship's roll motion may exhibit chaotic response under two different criteria (homoclinic and heteroclinic). The characteristics of and the relationship between the chaotic motion and capsize under the influence of noise will be investigated separately in each region.

Equations (3) and (4) can be rearranged and expressed as follows

$$\dot{X} = f_{1,2}(X) + g(X, \tau) \tag{9}$$

where $g(X, \tau)$ is considered as a perturbation to the Hamiltonian systems:

$$g(X, \tau) = \begin{Bmatrix} 0 \\ -\alpha x_2 - \alpha_q x_2|x_2| + A\cos(\Omega\tau + \Psi) + \eta(\tau) \end{Bmatrix} \tag{10}$$

By performing equivalent linearization on the quadratic drag force, eqn (10) can be simplified as:

$$g(X, \tau) = \begin{Bmatrix} 0 \\ -cx_2 + A\cos(\Omega\tau + \Psi) + \eta(\tau) \end{Bmatrix} \tag{11}$$

where cx_2 represents the equivalent linear damping force of the system. Equations (3) and (4) can then be cast in the form of stiffening and softening Duffing equations:

$$\ddot{x} + c\dot{x} - x + \beta_0^2x^3 = A\cos(\Omega\tau + \Psi) + \eta(\tau) \tag{12}$$

and

$$\ddot{x} + c\dot{x} + x - \beta_e^2x^3 = A\cos(\Omega\tau + \Psi) + \eta(\tau) \tag{13}$$

For lightly damped systems, the exact form of the damping mechanism is insignificant and it can be demonstrated that systems with both the quadratic damping force and the linearized damping force exhibit similar behavior. For convenient interpretation, only systems with the linearized damping force will be considered. Moreover, because the chaotic behavior has been widely investigated for both (deterministic) stiffening and softening forced Duffing systems, eqns (12) and (13) will be used to illustrate the characteristics of their corresponding stochastic ship roll motions.

3 METHODS OF ANALYSIS

In order to examine the characteristics of chaotic ship roll motions and capsize, several analysis procedures are

developed. The generalized Melnikov method is derived to provide criteria for the existence of the chaotic response in a noisy environment. The Markov process approach is used to depict the global stochastic behavior of the system's response via the evolutionary history of the PDF. Finally, the roll motion responses are simulated directly using numerical integration.

3.1 The generalized Melnikov method

The Melnikov function provides a quantitative tool to determine the existence of transverse intersections of homoclinic orbits and hyperbolic periodic orbits in the two-dimensional (roll angle and angular velocity) vector field. The presence of such intersections implies the existence of the chaotic response.[16–18] By a heuristic extension, the Melnikov method will be generalized herein for the ship's roll motion under periodic excitation with white noise.

Scaling the perturbations cx_2, $A\cos(\Omega\tau)$ and $\eta(\tau)$ by ϵ, eqn (9) then becomes

$$\dot{X} = f_{1,2}(X) + \epsilon g(X, \tau) \tag{14}$$

with $g(X, \tau)$ as expressed in eqn (11). As mentioned above, with different system parameters, two diverse chaotic dynamics (homoclinic and heteroclinic) for the roll motion may occur. Thus, a criterion for noisy chaotic roll motion in each case will be derived separately.

3.1.1 The homoclinic region

For relatively small roll motions (in the homoclinic region), the two homoclinic orbits can be represented by $q_{\pm}^{o1}(\tau)$ as explicit time functions:[16]

$$q_{\pm}^{o1}(\tau) = \left(\pm\frac{\sqrt{2}}{\beta_0\cosh(\tau)}, \mp\frac{\sqrt{2}\tanh(\tau)}{\beta_0\cosh(\tau)}\right) \tag{15}$$

In addition to the periodic wave excitation and linearized drag damping, the external random noise is considered as another source of perturbation to the homoclinic orbit. Due to the symmetry of the homoclinic orbits with respect to x_2 (Fig. 1), only the positive portion needs to be examined. The generalized Melnikov function is then given by

$$\begin{aligned} M_g^+(\tau_{1o}, \tau_{2o}) &= \int_{-\infty}^{\infty} f[q_+^{o1}(\tau)] \wedge g[q_+^{o1}(\tau); \tau_{1o}, \tau_{2o}]\mathrm{d}\tau \\ &= \frac{\sqrt{2}A\pi\Omega\cos(\Omega\tau_{10})}{\beta_0\cosh\left(\frac{\pi\Omega}{2}\right)} - \frac{4c}{3\beta_0^2} \\ &\quad - \frac{\sqrt{2}}{\beta_0}\int_{-\infty}^{\infty}\frac{\tanh(\tau)}{\cosh(\tau)}\eta(\tau+\tau_{2o})\mathrm{d}\tau \\ &= M_{\mathrm{d}}^+(\tau_{1o}) + M_{\mathrm{r}}^+(\tau_{2o}) \end{aligned} \tag{16}$$

where '+', as a superscript or subscript, implies the positive portion of the function. The first two terms in eqn (16), represented by $M_{\mathrm{d}}^+(\tau_{1o})$, correspond to the Melnikov function due to the deterministic perturbations, i.e. the periodic force and damping only. The last (integral) term, represented by $M_{\mathrm{r}}^+(\tau_{2o})$, corresponds to the Melnikov function due to the influence of Gaussian white noise. $M_{\mathrm{r}}^+(\tau_{2o})$ is a Gaussian random variable when the corresponding convolution integral is interpreted as linear filtering.[10] The transfer function of the linear filter, $q_+^{o1}(\tau)$, can be obtained through the Fourier transform:

$$F(\Omega) = \int_{-\infty}^{+\infty} q_+^{o1}(\tau)\mathrm{e}^{-\mathrm{i}\Omega\tau}\mathrm{d}\tau = \frac{-\mathrm{i}\Omega\pi}{\sqrt{2}\beta_0\cosh\left(\frac{\pi\Omega}{2}\right)} \tag{17}$$

The variance of $M_{\mathrm{r}}^+(\tau_{2o})$ can be obtained through the transfer function $F(\Omega)$:

$$\sigma_{M_{\mathrm{r}}}^2 = \int_{-\infty}^{\infty} F^2(\Omega)S_\eta(\Omega)\mathrm{d}\Omega \simeq \frac{13.15\kappa}{\beta_0^3} \tag{18}$$

where $S_\eta(\Omega)$ is the white noise spectral density, $2\pi\kappa$. In a noisy environment, the criterion for chaotic ship roll motion near the homoclinic orbits can be obtained by setting eqn (16) equal to zero:

$$M_{\mathrm{d}}^+(\tau_{1o}) + M_{\mathrm{r}}^+(\tau_{2o}) = 0 \tag{19}$$

Because $M_{\mathrm{r}}^+(\tau_{2o})$ is a Gaussian random variable, the criterion represented by eqn (19) can only be interpreted in a stochastic sense. The left-hand side of the equality is a Gaussian random variable with mean $M_{\mathrm{d}}^+(\tau_{1o})$ and variance σ^2. Moreover, since the Melnikov function renders a necessary condition for the existence of the chaotic response,[19] the criterion for noisy chaotic ship roll motion can be depicted via a mean-square representation:

$$\left\langle\left(\frac{4c}{3\beta_0^2}\right)^2\right\rangle = \left\langle\left(\frac{\sqrt{2}A\pi\Omega\cos(\Omega\tau_{1o})}{\beta_0\cosh\left(\frac{\pi\Omega}{2}\right)}\right)^2\right\rangle + \langle M_{\mathrm{r}}^2(\tau_{2o})\rangle \tag{20}$$

Then the following generalized (stochastic) Melnikov criterion, in terms of the parameters A, Ω, c, β_0, and κ, for chaotic response in the noisy forced small-amplitude ship roll motion can be obtained:

$$\left(\frac{4c}{3\beta_0^2}\right)^2 \le \frac{2A^2\pi^2\Omega^2}{\beta_0^2\cosh^2\left(\frac{\pi\Omega}{2}\right)} + \sigma_{M_{\mathrm{r}}}^2 \tag{21}$$

The mean-square representation of the critical surface for chaotic roll motion can be obtained when equality in eqn (21) is achieved. The criteria with or without noise disturbance in different parameter domains are represented by the dashed and solid lines, respectively, in Fig. 2.

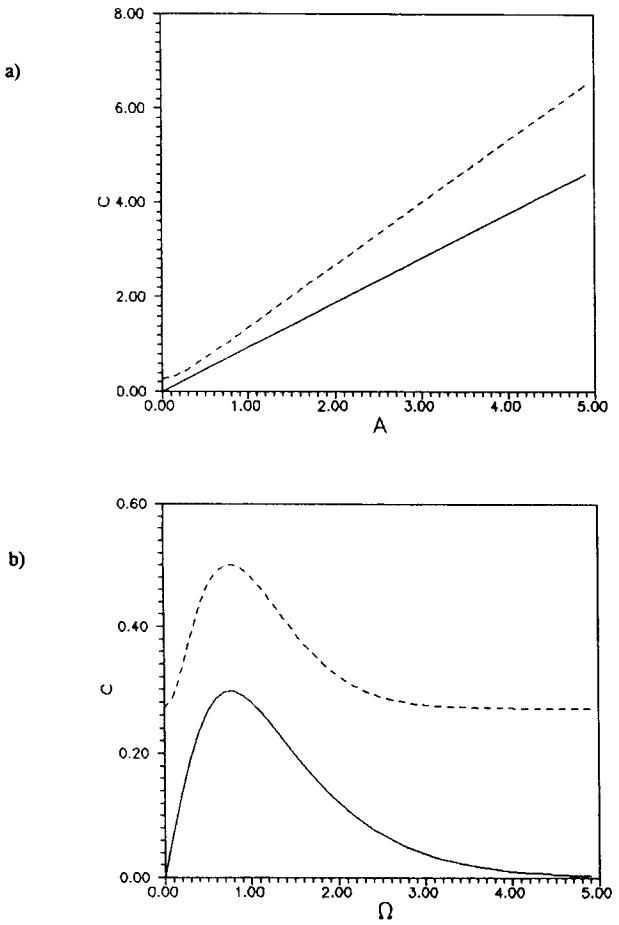

Fig. 2. Generalized Melnikov criterion for homoclinic chaos: (a) upper bound in c–A plane with $(\Omega, \beta_0, \Psi) = (1{\cdot}0, 1{\cdot}0, 1{\cdot}57)$; (b) upper bound in c–Ω plane with $(A, \beta_0, \Psi) = (0{\cdot}3, 1{\cdot}0, 1{\cdot}57)$. $\kappa = 0{\cdot}0$ and $0{\cdot}01$ for solid and dashed lines, respectively.

3.1.2 The heteroclinic region

For relatively large ship roll motions (in the heteroclinic region) the heteroclinic orbits can be represented by $q_{\pm}^{o2}(\tau)$ as an explicit time function:

$$q_{\pm}^{o2}(\tau) = \left(\pm \frac{1}{\beta_e} \tanh\left(\frac{\tau}{\sqrt{2}}\right), \pm \frac{1}{\sqrt{2}\beta_e \cosh^2\left(\frac{\tau}{\sqrt{2}}\right)} \right) \tag{22}$$

The corresponding generalized Melnikov function including stochastic effects is given by

$$M_g^+(\tau_{1o}, \tau_{2o}) = \frac{\sqrt{2}A\pi\Omega}{\beta_e \sinh\left(\frac{\pi\Omega}{2}\right)} \cos(\Omega\tau_{1o}) - \frac{2\sqrt{2}c}{3\beta_e^2} - \frac{1}{\sqrt{2}\beta_e} \int_{-\infty}^{\infty} \frac{\eta(\tau + \tau_{2o})}{\sinh^2\left(\frac{\tau}{\sqrt{2}}\right)} d\tau$$

$$= M_d^+(\tau_{1o}) + M_r^+(\tau_{2o}) \tag{23}$$

Again, '+', as a superscript or subscript, implies the positive portion of the function (Fig. 1). Similarly, the variance of $M_r^+(\tau_{2o})$ is given by

$$\sigma_{M_r}^2 = \int_{-\infty}^{\infty} F^2(\Omega) S_\eta(\Omega) d\Omega \simeq \frac{37{\cdot}22\kappa}{\beta_e^3} \tag{24}$$

where

$$F(\Omega) = \frac{2\pi\Omega}{\sqrt{2}\beta_e \sinh\left(\frac{\pi\Omega}{\sqrt{2}}\right)} \tag{25}$$

The mean-square representation of the stochastic criterion is given by

$$\left\langle \left(\frac{2\sqrt{2}c}{3\beta_e^2}\right)^2 \right\rangle = \left\langle \left(\frac{\sqrt{2}A\pi\Omega\cos(\Omega\tau_{1o})}{\beta_e \sinh\left(\frac{\pi\Omega}{\sqrt{2}}\right)} \right)^2 \right\rangle + \langle M_r^2(\tau_{2o}) \rangle \tag{26}$$

Then the following generalized (stochastic) Melnikov criterion in terms of the parameters A, Ω, c, β_e and κ for relatively large amplitude chaotic roll motion in a noisy environment can be obtained:

$$\left(\frac{2\sqrt{2}c}{3\beta_e^2}\right)^2 \leq \frac{2A^2\pi^2\Omega^2}{\beta_e^2 \sinh^2\left(\frac{\pi\Omega}{\sqrt{2}}\right)} + \sigma_{M_r}^2 \tag{27}$$

Again, the mean-square representation of the critical surface can be obtained when equality in eqn (27) is achieved. The criteria with and without noise disturbance in different parameter domains are represented by the dashed and solid lines, respectively, in Fig. 3.

It is noted that the positive correction term, $\sigma_{M_r}^2 = 13{\cdot}15\kappa/\beta_0^3$ (or $37{\cdot}22\kappa/\beta_e^3$), of the Melnikov function elevates the upper bound for possible chaotic response as shown in Fig. 2. Hence, noise could lower the threshold for chaotic ship roll motions, and enlarge the chaotic domain in the parameter space.

3.2 The Markov process approach

The behavior of the noisy forced ship roll motion under periodic excitation with Gaussian white noise can be approximated by a Markov process, the PDF of which satisfies a deterministic partial differential equation called the Fokker–Planck equation. The (temporal) solution to this partial differential equation can be obtained through a path integral solution procedure.[20–22] The numerical evaluation of the path integral solution procedure is performed based on the representation of the path sum.

3.2.1 The Fokker–Planck equation

The associated Fokker–Planck equations corresponding to small [eqn (12)] and large [eqn (13)] ship roll motions

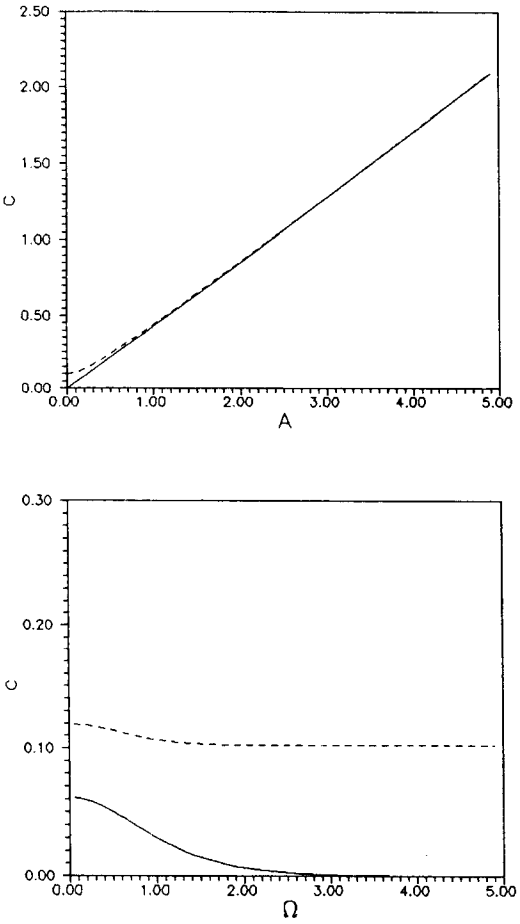

Fig. 3. Generalized Melnikov criterion for heteroclinic chaos: (a) upper bound in c–A plane with $(\Omega, \beta_e, \Psi) = (0{\cdot}5255, 1{\cdot}0, 0{\cdot}0)$; (b) upper bound in c–Ω plane with $(A, \beta_e, \Psi) = (0{\cdot}115, 1{\cdot}0, 0{\cdot}0)$. $\kappa = 0{\cdot}0$ and $0{\cdot}001$ for solid and dashed lines, respectively.

are:

$$\frac{\partial P(X,\tau)}{\partial \tau} = -\frac{\partial}{\partial x_1}\{x_2 P(X,\tau)\} - \frac{\partial}{\partial x_2}\{[-cx_2 + x_1 - \beta_0 x_1^3 + A\cos(\Omega\tau)] \times P(X,\tau)\} + \frac{\kappa}{2}\frac{\partial^2}{\partial x_2^2}P(X,\tau) \quad (28)$$

and

$$\frac{\partial P(X,\tau)}{\partial \tau} = -\frac{\partial}{\partial x_1}\{x_2 P(X,\tau)\} - \frac{\partial}{\partial x_2}\{[-cx_2 - x_1 + \beta_e x_1^3 + A\cos(\Omega\tau)]P(X,\tau)\} + \frac{\kappa}{2}\frac{\partial^2}{\partial x_2^2}P(X,\tau) \quad (29)$$

respectively, where $P(X, \tau)$ is the JPDF in (roll angle and angular velocity) phase space; $[x_2, -cx_2 + x_1 + \beta_0 x_1^3 + A\cos(\Omega\tau)]$ and $[x_2, -cx_2 - x_1 - \beta_e x_1^3 + A\cos(\Omega\tau)]$ correspond to the drift vectors; and $\kappa/2$ is the only non-zero entry in the two-by-two diffusion matrix (see Risken[21] for a detailed derivation). Periodic excitation appears in eqns (28) and (29) as a drift vector in both cases, hence the temporal solution of the PDF is periodic with a period $2\pi/\Omega$ in time according to the Floquet theorem.[23] In order to study the evolution of the JPDFs of the roll angle and angular velocity, the path integral solution will be employed.

3.2.2 The path integral solution

In the path integral solution procedure, the traveling path of the PDF in phase space is discretized into infinitesimal segments. Each segment represents a short-time propagation between two consecutive states in the corresponding Markov process. The short-time propagation is approximated by a time-dependent Gaussian distribution, called the short-time PDF, whose mean and variance is determined by the drift vector and the diffusion matrix, respectively. The PDF for the succeeding state can be determined through the propagation. Thus the probability for a desired state can be obtained by applying the short-time propagation iteratively.

The short-time PDFs, $G(X', X, \tau; d\tau)$, corresponding to eqns (28) and (29) are obtained as follows

$$G(X', X, \tau; d\tau) = (2\pi d\tau)^{-2} D_{22}^{-1/2} \times \exp\left[-\frac{d\tau}{2}D_{22}^{-1}\left(-cx_2 + x_1 - \beta_0 x_1^3 + A\cos(\Omega\tau) - \frac{x_2' - x_2}{d\tau}\right)^2\right]\delta\left(x_2 - \frac{x_1' - x_1}{d\tau}\right) \quad (30)$$

and

$$G(X', X, \tau; d\tau) = (2\pi d\tau)^{-2} D_{22}^{-1/2} \times \exp\left[-\frac{d\tau}{2}D_{22}^{-1}\left(-cx_2 - x_1 + \beta_e x_1^3 + A\cos(\Omega\tau) - \frac{x_2' - x_2}{d\tau}\right)^2\right]\delta\left(x_2 - \frac{x_1' - x_1}{d\tau}\right) \quad (31)$$

where X' and X represent the following and previous states, respectively. The PDF at the desired state can then be computed iteratively:

$$P(X,\tau) = \lim_{\substack{d\tau\to 0 \\ N\to\infty \\ Nd\tau\to\tau}} \prod_{i=0}^{N-1} \int \cdots \int \times \exp\left[-d\tau \sum_{j=0}^{N-1} G(X_{j+1}, X_j, \tau_j; d\tau) P(X_0, \tau_0)\right] dX_i \quad (32)$$

where $P(x_0, \tau_0)$ represents the initial condition (i.e. initial distribution) of the PDF. The path integral solution procedure yields the exact solution in the limit as $N \to \infty$ and $d\tau \to 0$ in eqn (32). A numerical approximation to the path integral solution is accomplished by

the path sum or discrete lattice representation of the path integral.[24] Based on the path integral solution algorithm, the propagation of the probability between consecutive states is described by the corresponding segment of the discretized mean path in probability space. The probability domains at the ends of each segment, i.e. the previous and following states, are discretized into a finite number of elements. Accordingly, the short-time PDF corresponding to the transition between consecutive states can be discretized into a transition tensor, and the PDF at the desired time can be achieved by iterating the short-time transition.

3.3 Direct numerical simulation

Realizations of the response of the noisy forced small and large amplitude ship roll motions can be obtained by directly integrating the governing differential equations [eqns (12) and (13)], e.g. using a Runge–Kutta fourth-order algorithm. Numerical representation of the Gaussian white noise selected in this study is based on Shinozuka's band-limited noise representation[25] which describes a Gaussian noise of zero mean, limited frequency bandwidth, and finite variance. It comprises a sum of harmonics with random frequencies and phase shifts with the noise level measured by σ^2. In this investigation, the number of harmonics is chosen to be 50 for an adequate representation of the Gaussian noise.

It is noted that in contrast to Shinozuka's Gaussian noise, ideal white noise is of infinite variance, and its strength is scaled by the noise intensity. However, Shinozuka's Gaussian noise model is adequate for demonstrating the characteristics of the system's response under the influence of ideal white noise. Thus, for this purpose, a numerical simulation with a Runge–Kutta fourth-order integration scheme along with Shinozuka's noise representation is employed.

4 STOCHASTIC INTERPRETATION OF THE NON-LINEAR SYSTEM'S BEHAVIOR

The ship roll motion is governed by two diverse dynamics in different phase domains, i.e. homoclinic and heteroclinic. The complete information about the system's behavior in each region can be depicted via the evolution of the associated PDFs. In order to preserve the characteristics of the system's responses, the intensity of the disturbance is kept small. The stability of chaotic ship roll motion in each region is illustrated stochastically. Moreover, the relationship between the chaotic motion near the heteroclinic orbits and capsize will be illustrated.

4.1 The homoclinic region

Chaotic ship roll motion may exist in the local homoclinic region when the Melnikov criterion [eqn (21)] is satisfied. The stochastic representation of one single chaotic attractor and coexisting chaotic and periodic attractors are demonstrated as follows.

4.1.1 The existence of a single chaotic attractor

Figure 4(a) shows an example of a deterministic chaotic roll motion in the homoclinic region represented by the Poincaré map. For the parameter set considered, there are no other attractors. In the presence of a small random disturbance to the external periodic excitation, the existence of this chaotic attractor can be identified via the JPDF on the Poincaré section [Fig. 4(b)], which is obtained by sampling the density at integer multiples of the excitation period. The imprint of the chaotic attractor is preserved and the PDF indicates the preferred locations of the trajectories in the average sense. The evolution of the PDF can be illustrated as well. The slightly disturbed ship roll motion is excited with a deterministic quiescent initial condition (0, 0) as shown in Fig. 5(a). The PDF starts spreading immediately and tends to cover and delineate the image of the chaotic attractor in just two evolutions [i.e. two periods of the deterministic external wave excitation, Fig. 5(b)]. The Poincaré section of the PDF achieves a steady state rather quickly. The steady-state chaotic attractor is clearly portrayed in 20 cycles [Fig. 5(c)].

4.1.2 The coexistence of chaotic and periodic attractors

Coexistence of attractors is one of the characteristics of non-linear systems. Figure 6(a) shows an example of the coexisting (homoclinic) chaotic and periodic attractors in the homoclinic region represented by the Poincaré map. These two distinctly different types of roll motion exist under the same system parameters with different initial conditions.

The PDF describes the complete information about the roll motion's behavior in the local homoclinic region, hence the coexistence of attractors can be demonstrated by this probabilistic representation,[13] as shown in Fig. 6(b). This representation can be performed by exciting the slightly disturbed ship roll system with deterministic initial conditions in the basin of the chaotic attractor and tracking the evolution of the PDF in state space. The PDF evolves from the quiescent position (0, 0) and spreads out to cover the chaotic attractor, as shown in Fig. 7(a) and (b). The steady state of the Poincaré section is achieved in about 20 cycles, as shown in Fig. 7(c), and the PDF depicts the two coexisting attractors clearly. The PDF represents the distribution of the ensemble of the trajectories and indicates the relative strength of the attractors. As shown in Fig. 7(c), a finite portion of the PDF is concentrated in the region of the periodic attractor. Based on a detailed examination of the numerical results, it is observed that the periodic and chaotic attractors are similar in strength. Therefore, sample

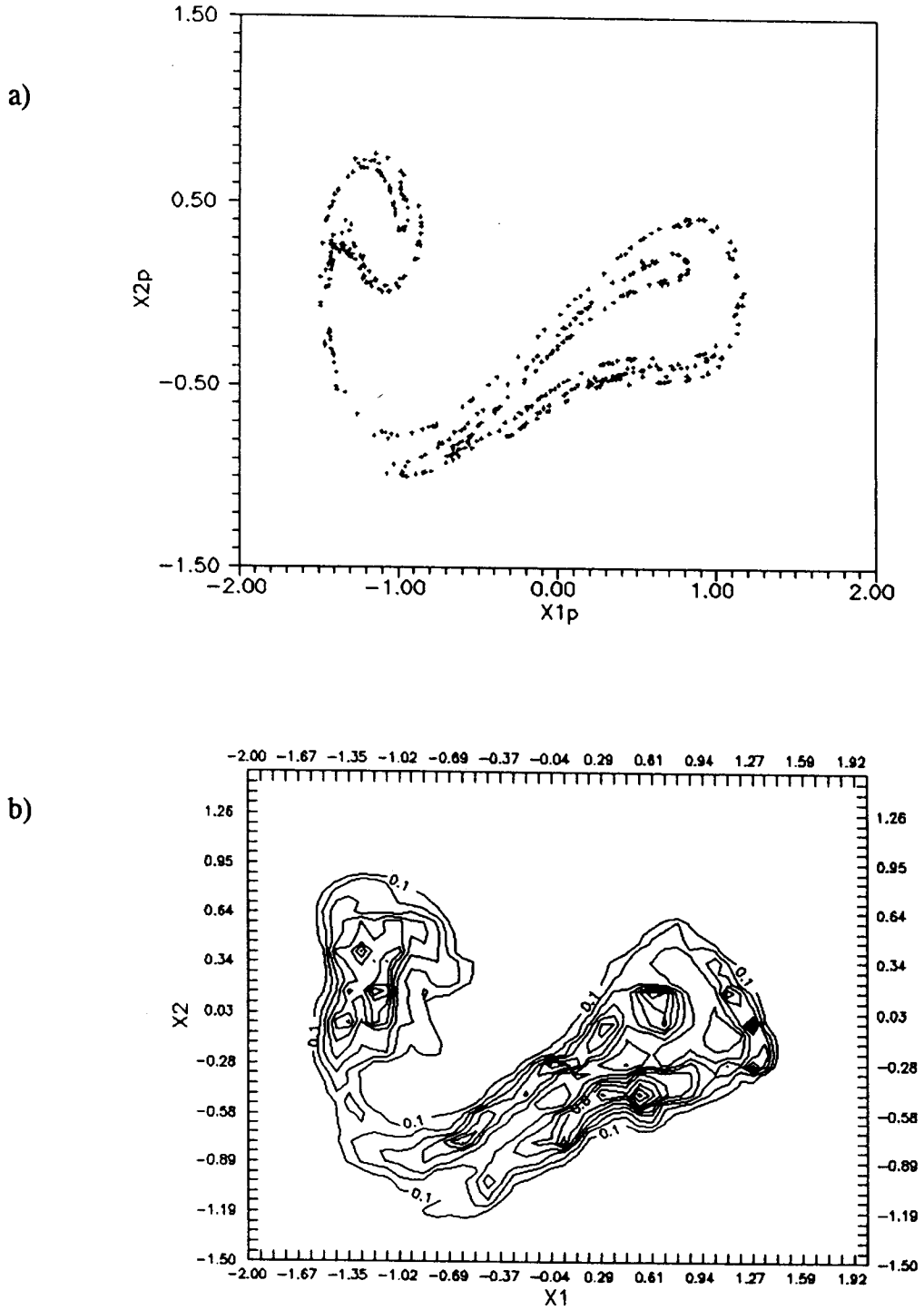

Fig. 4. Homoclinic chaotic attractor on Poincaré section: (a) Poincaré points from a single time history with $\kappa = 0{\cdot}0$, $A = 0{\cdot}3$; (b) probabilistic representation by the contour map of joint probability density with $\kappa = 0{\cdot}003$, $A = 0{\cdot}27$, and $(\Omega, c, \beta_0, \Psi) = (1{\cdot}0, 0{\cdot}185, 1{\cdot}0, 1{\cdot}57)$.

paths of the roll motion may drift in and out of both attractors and exhibit periodic as well as chaotic roll motions when noise is present. Moreover, the PDF elucidates the overall steady-state stochastic behavior in the parameter space, and the initial conditions become insignificant when describing the global long-term behavior. This contrasts with the sensitivity to the initial conditions of the sample paths of a single (deterministic) chaotic trajectory and demonstrates the smoothing effect of low-intensity random noise disturbance.

The slight difference in parameters is noted in Fig. 6. The shift in the threshold of the different response states is caused by the presence of noise which is indicated in the Melnikov criterion. The approximation in the path integral solution procedure introduces additional

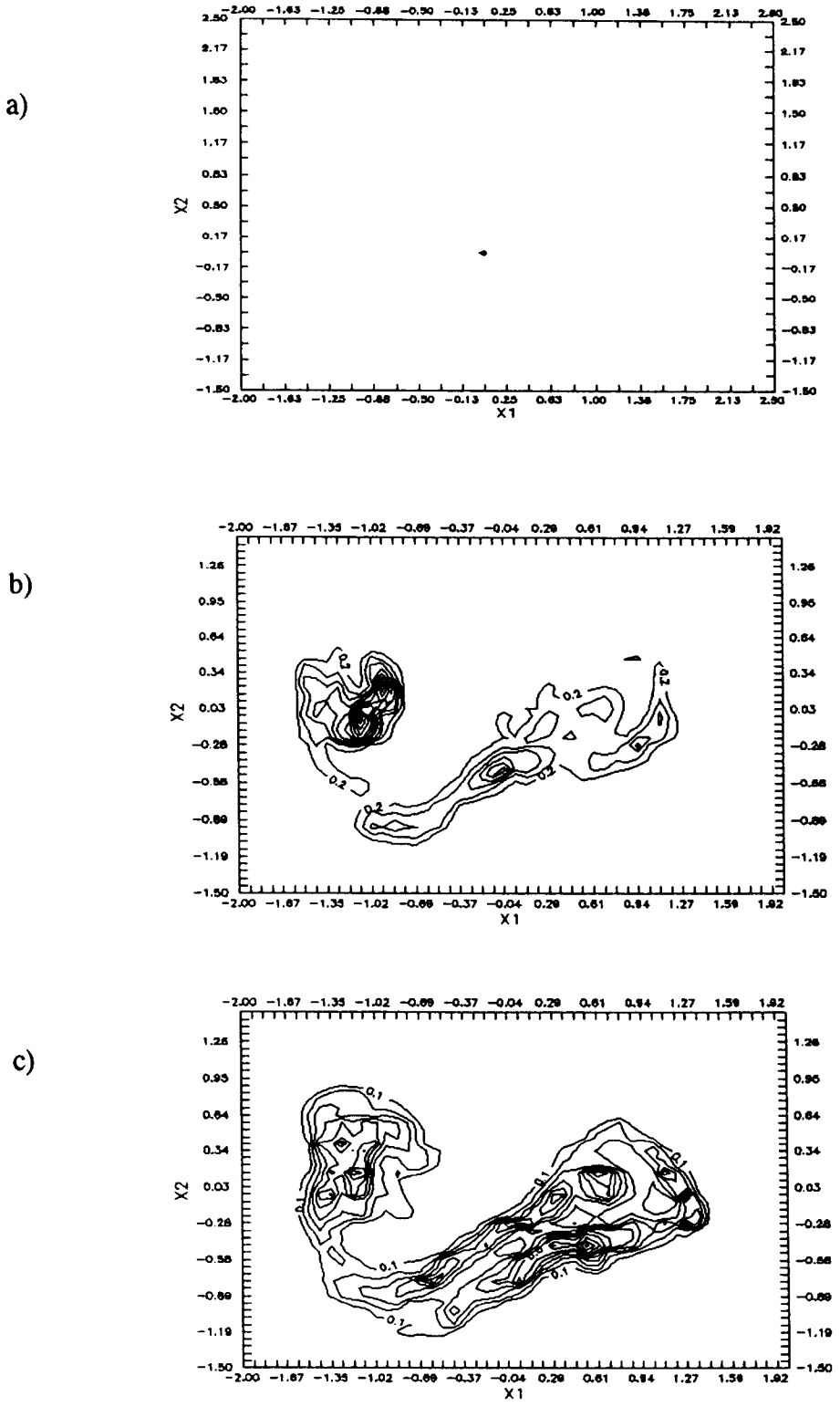

Fig. 5. Evolution of joint probability density: contour map of probability density at (a) initiation at (0·0, 0·0); and at (b) the 2nd and (c) the 20th cycles of the forcing period. $(A, \Omega, c, \beta_0, \Psi) = (0{\cdot}25, 1{\cdot}0, 0{\cdot}185, 1{\cdot}0, 1{\cdot}57)$.

uncertainties as the number of iterations increases, which could shift the threshold further. However, the resulting PDFs still fully reflect the global behavior of the ship's roll motion and provide a strong indication of the response characteristics.

4.2 The heteroclinic region

For relatively large amplitude ship roll motions (in the local homoclinic region) the ship capsizes when the response trajectory escapes out of the heteroclinic orbits

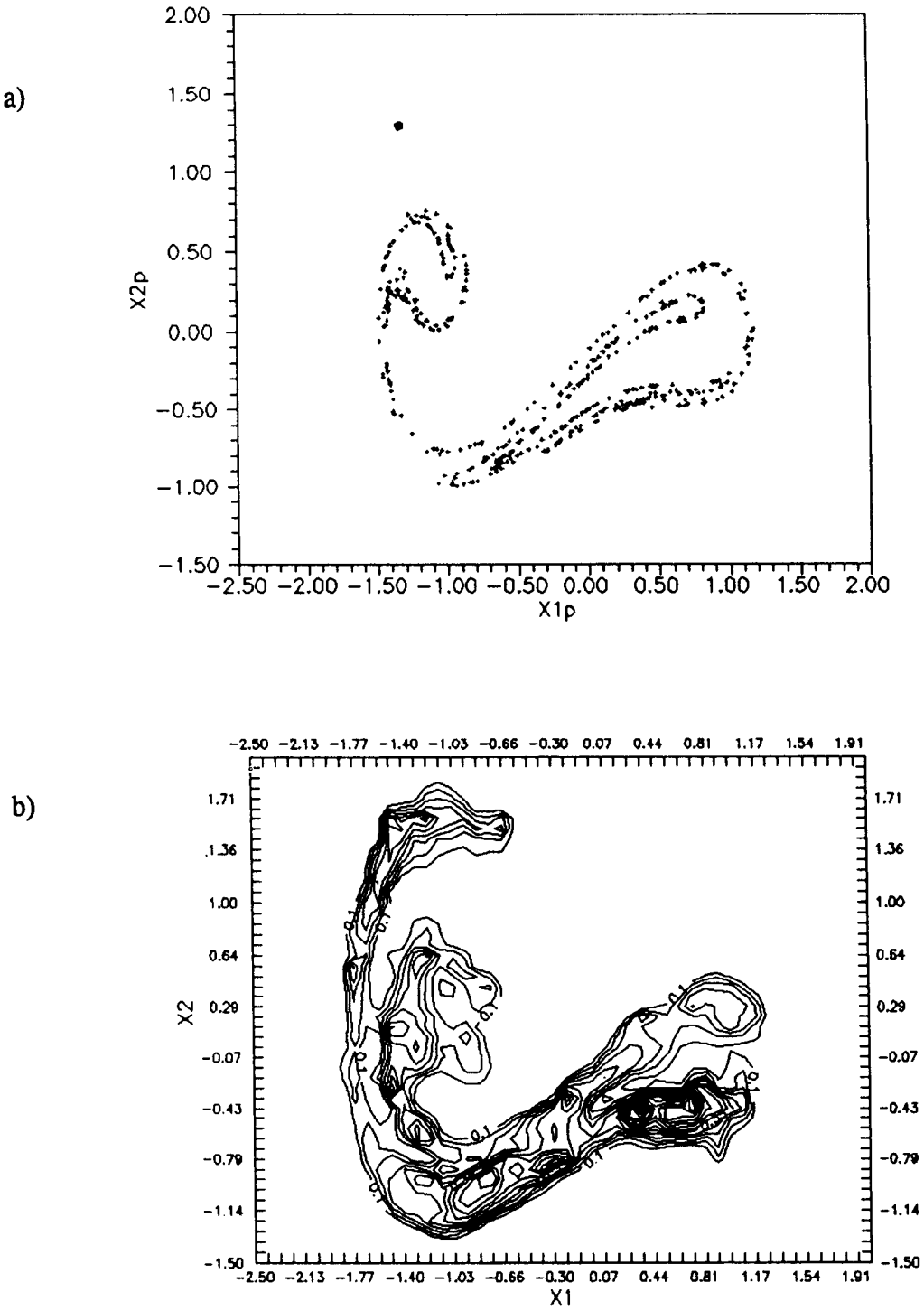

Fig. 6. Coexisting homoclinic chaotic and periodic attractors on the Poincaré section: (a) Poincaré points from a single time history with $\kappa = 0{\cdot}0$, $c = 0{\cdot}15$; (b) probabilistic representation by the contour map of joint probability density with $\kappa = 0{\cdot}003$, $c = 0{\cdot}185$. (A, Ω, β_0, Ψ) = (0·3, 1·0, 1·0, 1·57).

and diverges with time. The response may also reveal chaotic behavior when the stochastic Melnikov criterion [eqn (27)] is met. With a small disturbance added to the periodic excitation, the relationship between the chaotic ship roll motion near the heteroclinic orbits and capsize can be demonstrated stochastically.

Near the heteroclinic orbits, an example of chaotic roll motion coexisting with periodic motion in a deterministic state is shown in Fig. 8(a). By adding a weak random noise to the excitation, the PDF of the roll motion response in the local heteroclinic region can be obtained as described in the previous sections and shown in Fig. 8(b). On the Poincaré section, no steady-state solution can be achieved for the PDF. The boundaries of the coexisting attractors are bridged by the noise, and divergence of the PDF

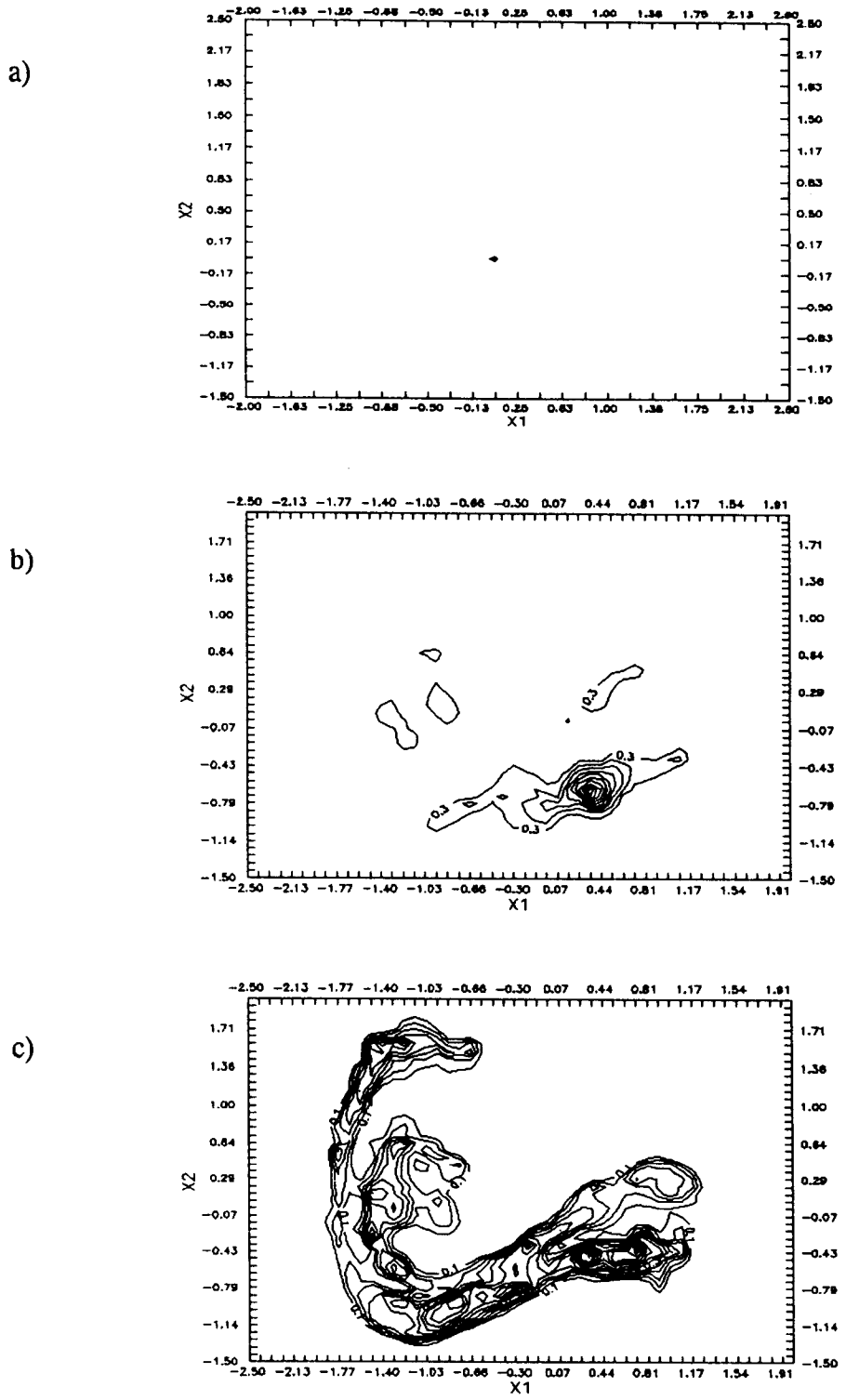

Fig. 7. Evolution of joint probability density: contour map of probability density at (a) initiation at (0·0, 0·0); and at (b) the 2nd and (c) the 20th cycles of the forcing period. (A, Ω, c, β_0, Ψ)=(0·3, 1·0, 0·185, 1·0, 1·57).

indicates the dominant attracting strength of capsizing relative to the other bounded (chaotic and periodic) motions. Therefore, in the neighborhood of the heteroclinic orbits with the presence of noise, all the motion trajectories will eventually lead to capsize.

5 NOISE EFFECTS ON RESPONSE BEHAVIOR

As demonstrated, the boundaries of the domains of the periodic and chaotic ship roll motion attractors are bridged when the system is disturbed by random noise. Thus the intensity of the random noise can be

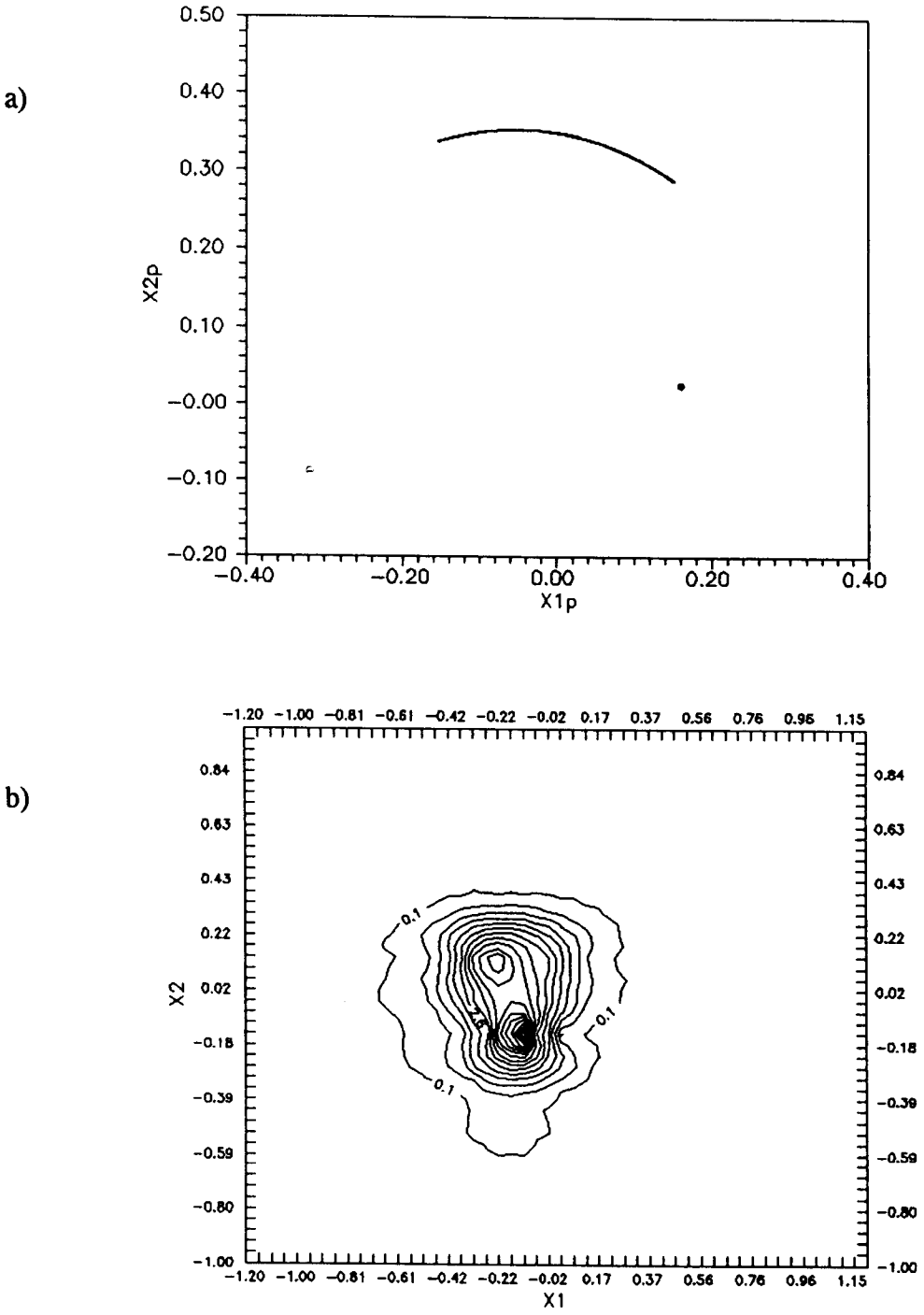

Fig. 8. Coexisting heteroclinic chaotic and periodic attractors: (a) Poincaré map (5000 points) from a single time history with $\kappa = 0{\cdot}0$; (b) non-stationary joint probability density sampled at $\tau = 8$. $(A, \Omega, c, \beta_e, \Psi) = (0{\cdot}115, 0{\cdot}5255, 0{\cdot}4, 4{\cdot}0, 0{\cdot}0)$.

considered as a control parameter. In this study, the homoclinic and heteroclinic regions of the ship roll motion in phase space are assumed to be sufficiently far apart from each other so that each region can be investigated separately. The influence of noise on chaotic behavior and capsize in both homoclinic and heteroclinic regions can be examined by varying its intensity and is illustrated via the transient and steady-state PDFs. For both the homoclinic and heteroclinic regions, modifications of the chaotic domain due to noise as depicted by the associated generalized Melnikov functions, and the transitions between different response states, will be demonstrated through numerical simulations. The relationship between chaotic ship roll motion and capsize in the heteroclinic region will be considered as an extreme excursion problem with the time-averaged PDF as an invariant measure.

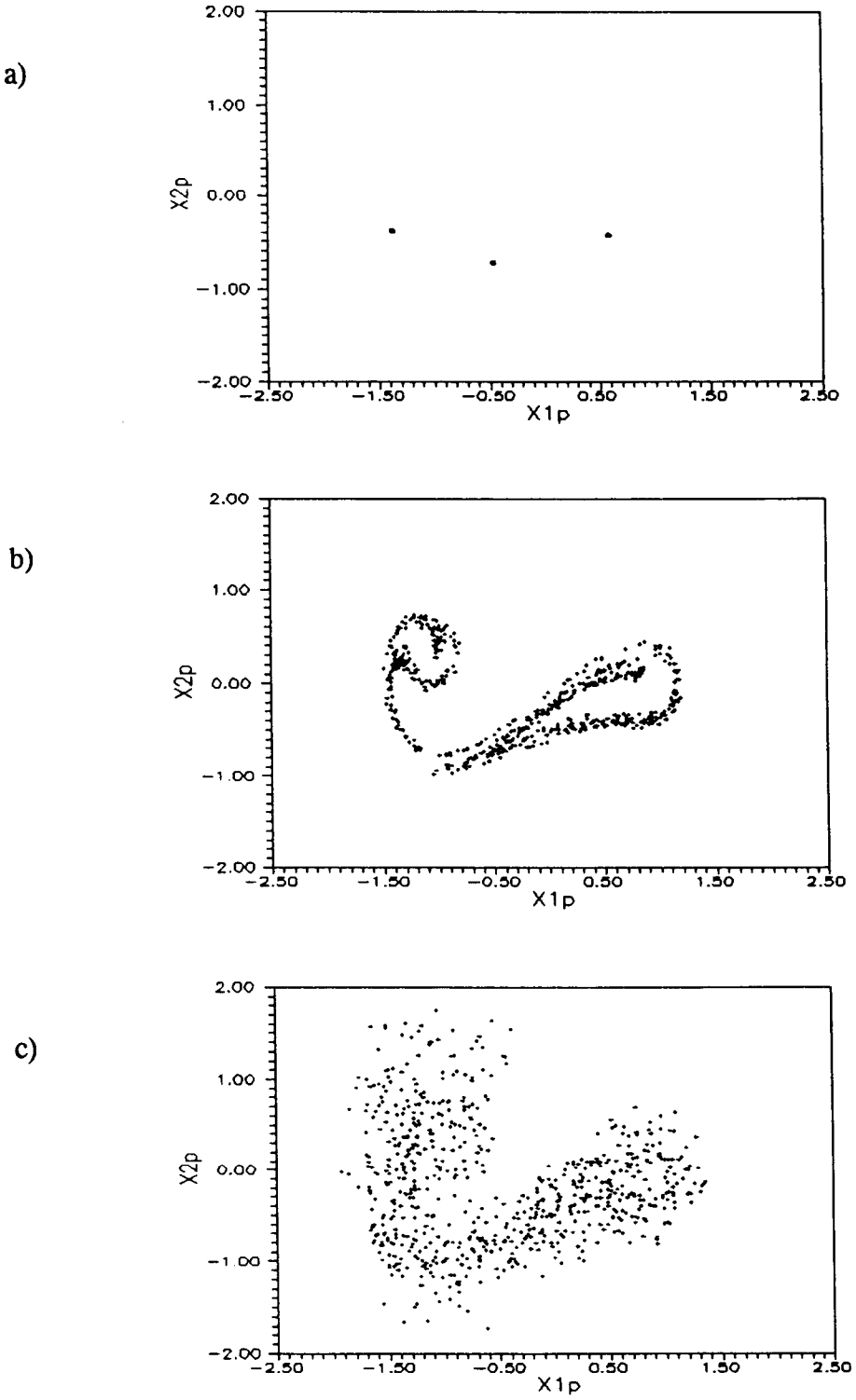

Fig. 9. Noise-induced transition in the homoclinic domain (direct numerical simulations): (a) periodic response with $\sigma^2 = 0{\cdot}0$; (b) noise-induced chaotic response with $\sigma^2 = 0{\cdot}0016$; (c) random-like response with $\sigma^2 = 0{\cdot}16$. $(A, \Omega, c, \beta_0, \Psi) = (0{\cdot}28, 1{\cdot}0, 0{\cdot}185, 1{\cdot}0, 1{\cdot}57)$.

5.1 Noise-induced transitions in the ship roll motion

5.1.1 The homoclinic region

Near the homoclinic region, due to the fact that the ship roll motion trajectories are bounded by the potential barriers formed by the heteroclinic orbits, as long as the disturbance is weak, all the responses can be considered to be of finite amplitude. As delineated analytically by the generalized stochastic Melnikov function, the presence of weak noise can expedite the occurrence of chaotic roll motion response, which is demonstrated in Fig. 9(a) and (b). Figure 9(a) shows that the response

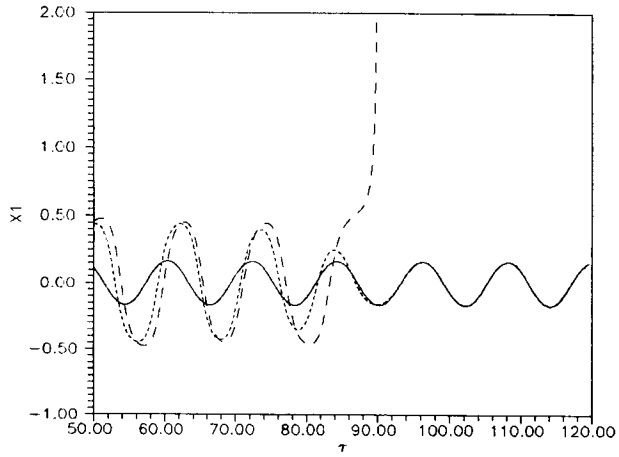

Fig. 10. Noise-induced transition in the heteroclinic domain (time histories from direct numerical simulations): solid, short-dashed and long-dashed lines represent the responses from the system with $\sigma^2 = 0{\cdot}0$, $0{\cdot}004^2$, and $0{\cdot}005^2$, respectively. (A, Ω, c, β_e, Ψ) = (0·115, 0·5255, 0·4, 4·0, 0·0).

without noise disturbance is periodic (in fact, one-third subharmonic). Figure 9(b) shows that chaotic roll motion is induced by the presence of external noise, which implies that noise enlarges the chaotic domain in the parameter space. With stronger noise intensity, the response appears random as shown in Fig. 9(c). Thus, with noise intensity as a control parameter, in the neighborhood of the homoclinic chaotic domain, the chaotic response appears to be an intermediate state between periodic and random roll motion responses.

5.1.2 The heteroclinic region

Transitions induced by the external noise can be observed in the heteroclinic region as shown in Fig. 10. The solid line represents a periodic roll motion response without noise in the excitation ($\sigma^2 = 0{\cdot}0$). The periodic response stays bounded under the presence of a low-intensity external disturbance (short-dashed line, $\sigma^2 = 0{\cdot}004^2$). However, it diverges to the capsizing domain when the intensity of the disturbance is slightly increased (long-dashed line, $\sigma^2 = 0{\cdot}005^2$). Thus it can be concluded that the heteroclinic dynamics of the roll motion is very sensitive to the magnitude of the intensity of the external noise disturbance. Because of the noise-induced bridging effect (which bridges the boundaries of all the coexisting attractors) and the relatively weak strength of the chaotic attractor, no chaotic roll motion response near the heteroclinic orbits can be observed even with small disturbances (see previous section). Thus, due to the instability of the response behavior in the heteroclinic region, roll motion trajectories close to the heteroclinic orbit will eventually diverge from the bounded motion to the capsizing domain under the presence of a small disturbance.

5.2 Noise effects on chaotic roll motions

5.2.1 Chaotic roll response in the homoclinic region

5.2.1.1 A single chaotic attractor. The noise effect on a single roll motion chaotic attractor can be demonstrated by varying the external noise intensity. When the roll motion near the homoclinic orbits is disturbed by noise, the stochastic properties of the chaotic attractor can be examined via the PDF. As shown in Fig. 11(a), with a weak noise intensity ($\kappa = 0{\cdot}003$), the clear portrait of the boundary of the JPDF implies that the disturbed roll motion trajectories stay inside the chaotic attractor. By increasing the noise intensity ($\kappa = 0{\cdot}02$), the shape of the JPDF becomes blurry [Fig. 11(b)], which implies that the boundary of the chaotic attractor has deteriorated and the trajectories may visit the vicinal area outside the attractor. This noise-induced smoothness of the PDF indicates that the preference of a (jagged) amplitude distribution of the chaotic roll motion response becomes ambiguous. In other words, the noise decreases the 'orderliness' of the chaotic roll motion and the response exhibits a more random-like behavior. Further increase in the noise intensity may result in large excursions of the roll motion amplitude leading to capsize, which is not considered in the local homoclinic region. Capsize induced by large noise disturbances to the chaotic response near the homoclinic orbits will be discussed as an extreme excursion problem later.

5.2.1.2 Coexisting chaotic and periodic attractors. The distribution of the PDF of the roll motion response in phase space indicates the relative strengths of the corresponding (periodic and/or chaotic) attractors. Recall that the steady state is achieved by solving the transient Fokker–Planck equation for long times using the path-integral method with a quiescent initial condition [i.e. (0, 0)]. For ship roll motion under deterministic excitation (i.e. without noise), with a quiescent initial condition, the response converges to a chaotic attractor only (see Section 4.1.2). The coexisting periodic attractor can only be reached with non-quiescent initial conditions.

The steady state of the PDF for the roll motion response with a small disturbance ($\kappa = 0{\cdot}001$) is shown in Fig. 12(a). It indicates that, even with such a small disturbance, the periodic attractor can be reached from quiescent initial condition, thus the attracting basins of the periodic and chaotic attractors in phase space have been bridged. Because of the weak noise intensity, only partial information on the chaotic attractor is depicted by the corresponding JPDF. The exact shape of the chaotic attractor cannot be clearly identified as compared to that of Fig. 6(b).

However, when the noise intensity increases ($\kappa = 0{\cdot}003$), in the steady state [Fig. 12(b)], it is observed

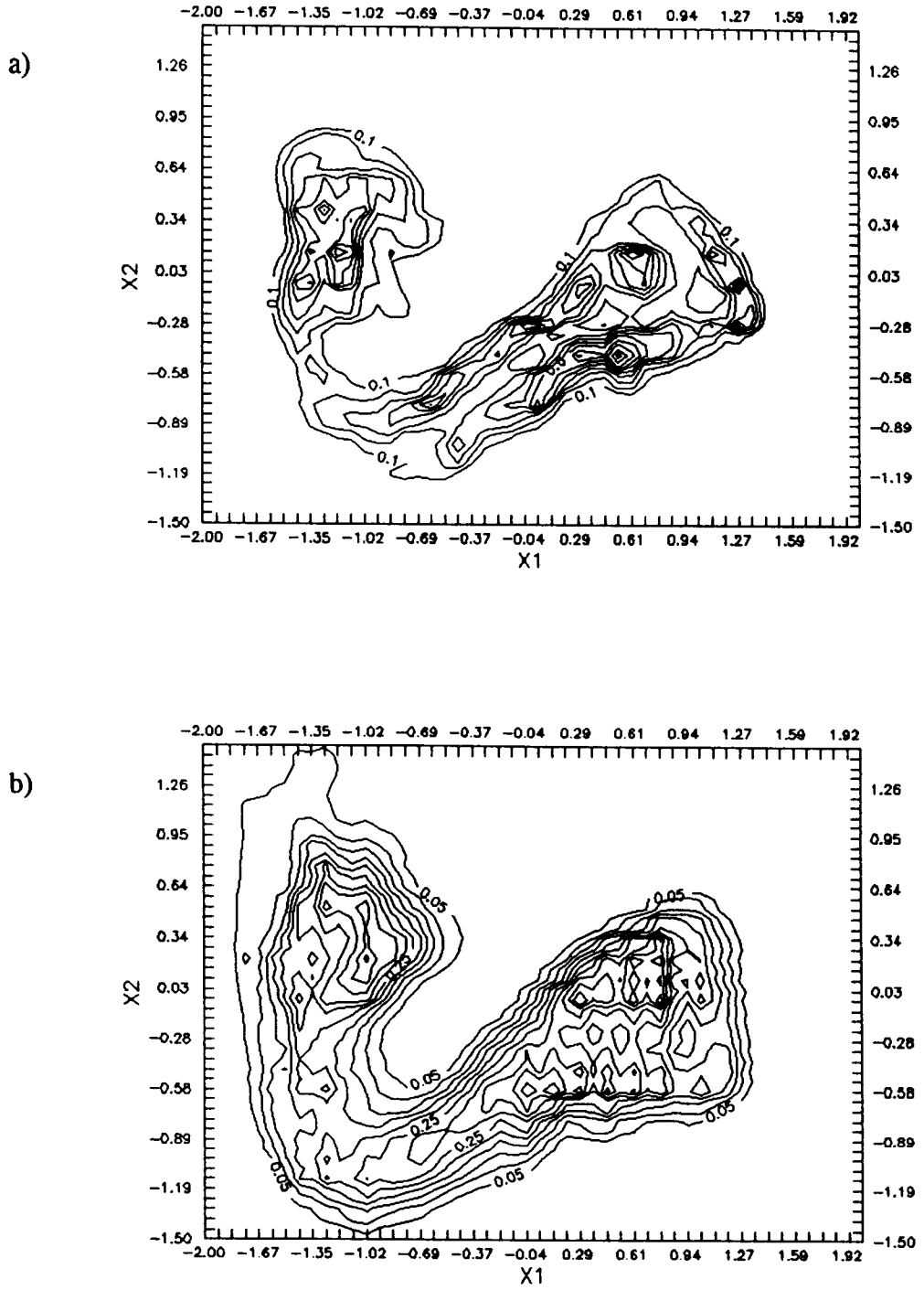

Fig. 11. The transition in the probability density on the Poincaré section under the influence of noise: contour maps of probability density with (a) $\kappa = 0{\cdot}003$; (b) $\kappa = 0{\cdot}02$. $(A, \Omega, c, \beta_0, \Psi) = (0{\cdot}27, 1{\cdot}0, 0{\cdot}185, 1{\cdot}0, 1{\cdot}57)$.

that the relative strength of the chaotic attractor also increases. The global information about the dynamical system is now fully depicted by the JPDF. This can be explained by the fact that as the basins of attraction for the periodic and chaotic attractors overlap further, it becomes easier for the roll motion trajectories to revisit the chaotic attractor from the stronger periodic attractor. When the noise intensity increases further ($\kappa = 0{\cdot}007$), the roll motion behavior appears random, as shown in Fig. 12(c), and the possibility of capsize should be considered.

Thus it is observed that the strength of the chaotic attractor (relative to the periodic attractor) is enhanced by the presence of low-intensity random noise. Hence, it may be easier to identify the chaotic characteristics and global information over the entire phase space of the

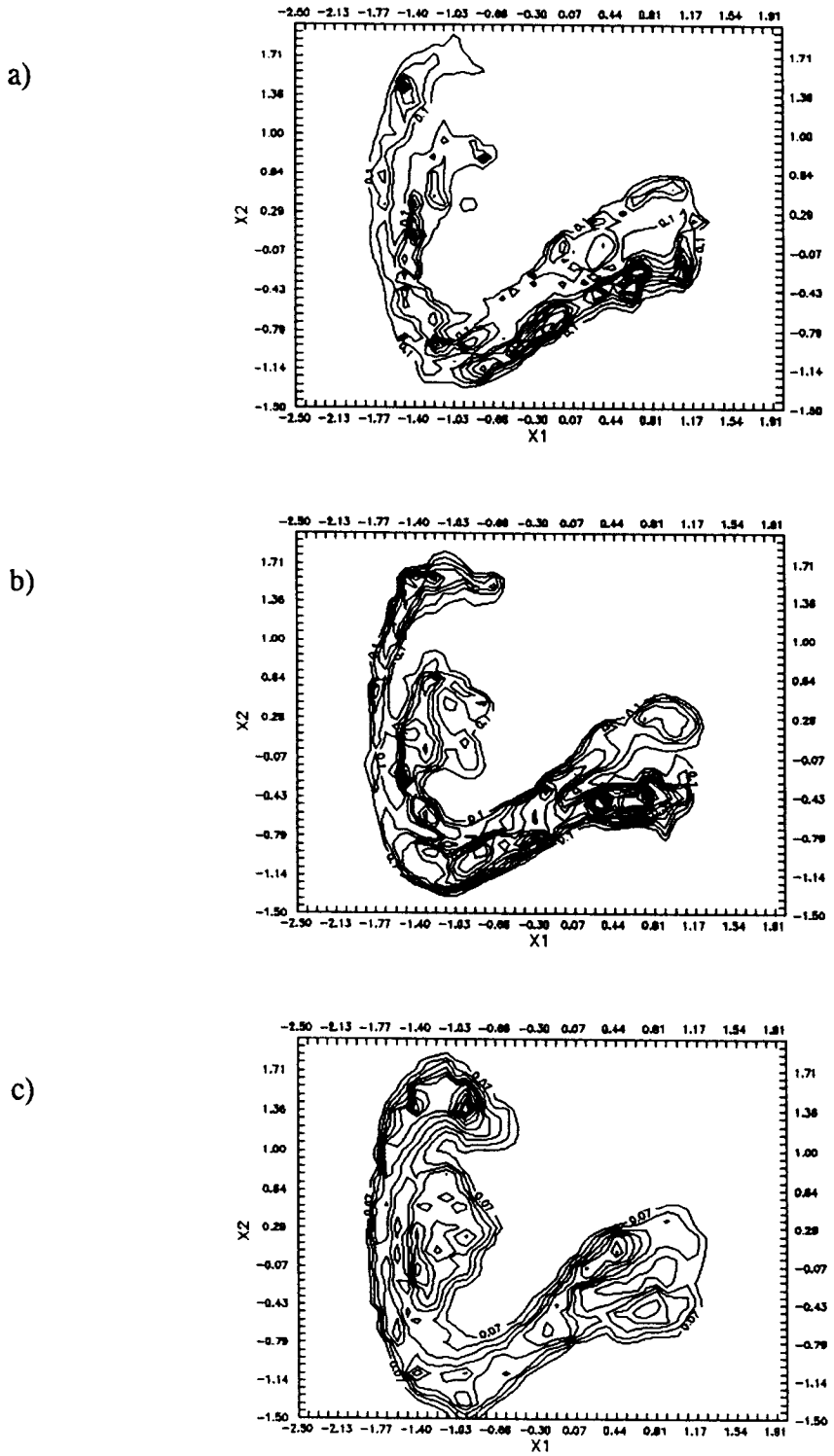

Fig. 12. The transition in the probability density on the Poincaré section under the influence of noise: contour maps of probability density with (a) $\kappa = 0{\cdot}001$; (b) $\kappa = 0{\cdot}003$; (c) $\kappa = 0{\cdot}007$. $(A, \Omega, c, \beta_0, \Psi) = (0{\cdot}3, 1{\cdot}0, 0{\cdot}185, 1{\cdot}0, 1{\cdot}57)$.

ship roll motion via stochastic analysis by adding an adequate amount of disturbance in an otherwise deterministic system.

5.2.2 Chaotic roll response in the heteroclinic region

As demonstrated in previous sections, the chaotic roll motion response in the heteroclinic region diverges, leading to capsize of the ship, when an external disturbance is applied. No steady-state solution for the associated PDF can be obtained due to the fact that the basins of all coexisting attractors are bridged by the noise, and among them, the capsizing attractor is of the greatest strength.

In a deterministic state (near the heteroclinic orbits),

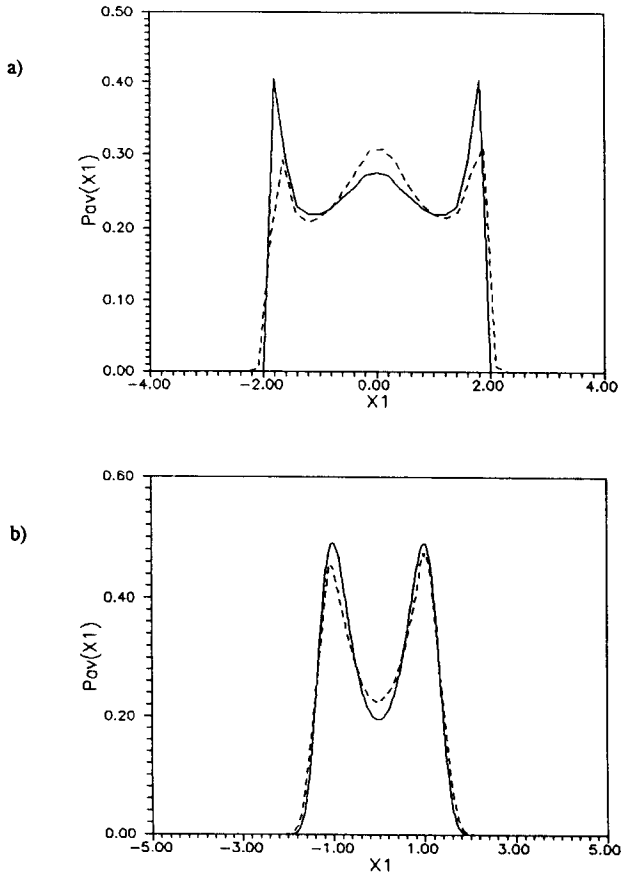

Fig. 13. The invariant measure for deterministic and random dynamics: (a) deterministic, exact solution with $(A, \kappa) = (0{\cdot}5, 0{\cdot}0)$ and approximation with $(A, \kappa) = (0{\cdot}5, 0{\cdot}001)$; (b) random, exact solution and approximation with $(A, \kappa) = (0{\cdot}0, 0{\cdot}1)$. The exact solution and the approximation from the path integral procedure are represented by solid and dashed lines, respectively. $(\Omega, c, \beta_0, \Psi) = (1{\cdot}0, 0{\cdot}185, 1{\cdot}0, 1{\cdot}57)$.

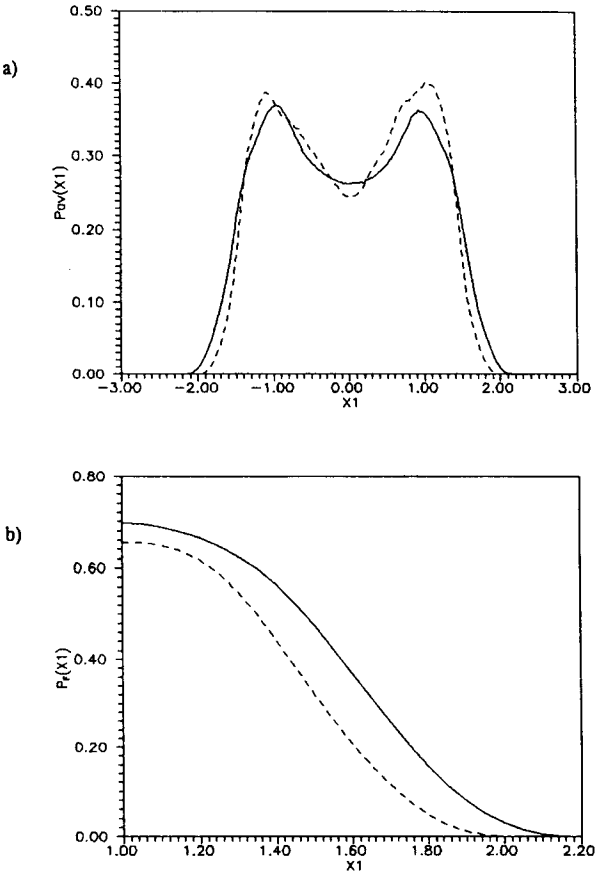

Fig. 14. The invariant measure and probability of extreme values. (a) The invariant measure for various noise intensities. (b) The corresponding probabilities of large displacements. The dashed and solid lines represent the cases with $\kappa = 0{\cdot}02$ and 0·07, respectively. $(A, \Omega, c, \beta_0, \Psi, \tau_n) = (0{\cdot}27, 1{\cdot}0, 0{\cdot}185, 1{\cdot}0, 1{\cdot}57, 10{\cdot}0)$.

the phenomenon that different initial conditions may lead to chaotic roll motion or capsize could be explained by the overlapping of the boundaries of the basins of attraction[3] or by the lobe dynamics.[2] However, in a stochastic state, the boundaries of all basins of attraction are bridged and the sensitivity to the initial conditions becomes insignificant. Thus, a ship will capsize eventually when the associated roll motion response trajectory visits the heteroclinic region. Therefore, by considering the heteroclinic region as the 'unsafe region', the probability of capsize stemming from disturbed chaotic roll motion response near the homoclinic orbits can be evaluated.

5.3 Distribution of the maximum response

The effects of weak random noise on single and coexisting attractors in the local homoclinic region of the roll angle and velocity phase space were examined in the previous two sections. Noise-induced smoothness in the PDFs indicates that probability mass may leak out of the boundaries of the attractors. Thus, albeit at a low probability level, the associated roll motion trajectories may visit the heteroclinic region and eventually lead to capsize. The probability of capsize of the associated deterministic bounded responses due to the presence of noise can be estimated via a time-averaged PDF as an invariant measure.

5.3.1 Time-averaged probability density function

As mentioned in Section 3, the steady-state JPDF of the roll angle and angular velocity state-space is periodic. Thus the PDF on the Poincaré section exhibits an invariant property (see Figs 4–7, 11 and 12). This periodicity can be removed by taking the average of the PDF over a suitably large duration to form a time-averaged PDF [15,26] which can be defined as the invariant measure for all dynamics, i.e. deterministic, chaotic and random:

$$P_{\mathrm{av}}(X) = \frac{1}{t_{\mathrm{n}}} \int_0^{t_{\mathrm{n}}} P(X, t)\mathrm{d}t \tag{33}$$

and the invariant measure on x_1 (i.e. the marginal PDF)

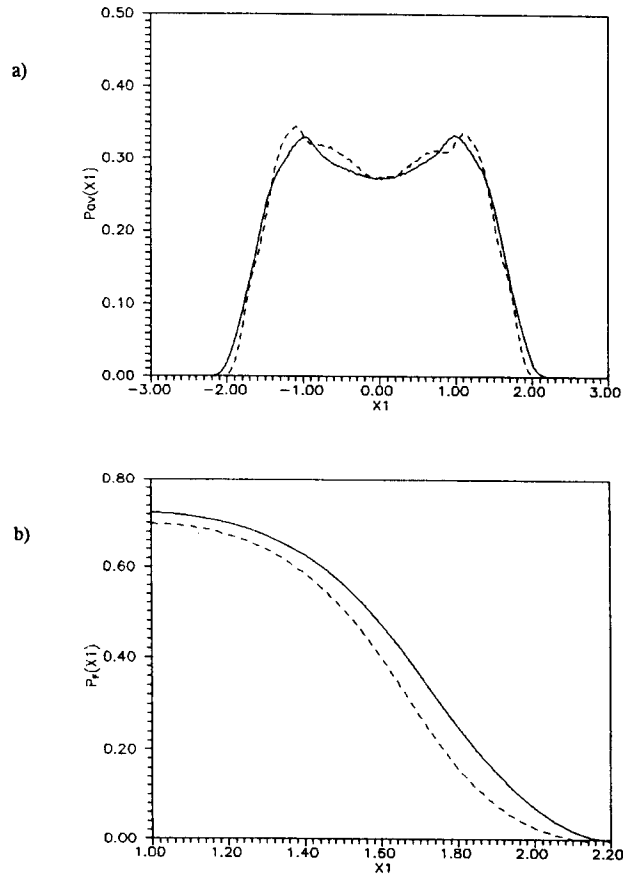

Fig. 15. The invariant measure and probability of extreme values. (a) The invariant measure for various noise intensities. (b) The corresponding probabilities of large displacements. The dashed and solid lines represent the cases with $\kappa = 0{\cdot}02$ and $0{\cdot}07$, respectively. $(A, \Omega, c, \beta_0, \Psi, \tau_n) = (0{\cdot}3, 1{\cdot}0, 0{\cdot}185, 1{\cdot}0, 1{\cdot}57, 10{\cdot}0)$.

is

$$P_{av}(x_1) = \int_{-\infty}^{\infty} P_{av}(x_1, x_2)\mathrm{d}x_2 \tag{34}$$

Figure 13(a) represents the (time-averaged) invariant measures of the periodic (deterministic) (solid line) and slightly disturbed (stochastic) (dashed line) ship roll motions. The deterministic results are obtained numerically from the statistics of the periodic attractor, and the stochastic results are obtained via the path-integral procedure. The similarity in the invariant measures of these two cases indicates that the deterministic state may be obtained in the limit as the noise intensity approaches zero.

For purely random excitation with no periodic component, the exact theoretical solution of the PDF for the corresponding Fokker–Planck equation[27] and the approximated invariant measure from the Markov process approach obtained using the path-integral procedure are compared in Fig. 13(b). The figure shows good agreement between the two solutions in general. Thus the two figures [Fig. 13(a) and (b)] indicate that the invariant properties of the ship roll motion can be revealed by the time-averaged PDF (invariant measure). Also, the path integral solution procedure can provide a good approximation which is especially accurate at the tail (a quality essential for extreme excursion problems).

By employing Rice's formula,[28] the mean up-crossing frequency of the roll motion can be evaluated:

$$\mu_{x_1}^{+}(x_d) = \int_0^{\infty} x_2 p_{av}(x_d, x_2)\mathrm{d}x_2 \tag{35}$$

Moreover, by adopting the assumption of statistically independent large-amplitude up-crossings (which leads to Poisson-distributed crossing events[29]) the asymptotic approximation of the probability that x_1 exceeds a specified (high) level x_d during time τ_n is given by:

$$p_F(x_d, \tau_n) = 1 - \exp[-\mu_{x_1}^{+}(x_d)\tau_n] \tag{36}$$

The cases with a single chaotic attractor [see Fig. 4(b)] and coexisting periodic and chaotic attractors [see Fig. 6(b)] under the influence of noise with various intensities are examined. Figure 14(a) shows the time-averaged PDF for the noisy single chaotic attractor corresponding to Fig. 4(b), but with a relatively high noise intensity ($0{\cdot}02$ for the dashed line and $0{\cdot}07$ for the solid line). The corresponding probabilities for extreme excursions ($\tau_n = 10$) are shown in Fig. 14(b).

Also, as demonstrated in the previous section, the external noise bridges the domains of attraction of the coexisting periodic and chaotic ship roll motions and its intensity governs the relative strengths of the attractors. Hence, both attractors should be considered when the extreme excursion is estimated. In regard to the coexisting attractors, the time-averaged PDF of the roll motion response and the corresponding probabilities of the extreme excursions ($\tau_n = 10$) are shown in Fig. 15(a) and (b), respectively.

Note that the probability of a large displacement is increased as the noise intensity increases for both the single- and the coexisting-attractor cases. However, the influence of the presence of noise is more pronounced for the case with the single chaotic attractor [Fig. 14(b)] than that for the case of coexisting attractors [Fig. 15(b)]. The existence of a coexisting periodic attractor enlarges the attraction domain [e.g. see Fig. 6(b)] and flattens the invariant measure [c.f. Figs 14(a) and 15(a)]. This may cause the variation of noise intensity to appear less significant in terms of the probability of large displacement in the coexisting-attractor case [Fig. 15(b)] than in the single chaotic attractor case [Fig. 14(b)].

6 CONCLUDING REMARKS

This paper examines the periodic, chaotic and capsizing responses of a ship's roll motion from a stochastic point of view. With the intensity of an external random noise source as the control parameter, the characteristics of

and the relationships among these responses are demonstrated, and the associated extreme value distribution is examined. The main conclusions are as follows.

1. The ship's roll motion is governed by two diverse dynamic regions—homoclinic and heteroclinic. For both regions, stochastic analytical criteria for noisy chaotic motions have been derived in terms of a generalized Melnikov function which takes into account the presence of additive white noise. The noise enlarges the domain of the chaotic response in parametric space, and chaotic motions may occur in this expanded region.
2. The local behavior of the chaotic roll motions near the homoclinic or heteroclinic regions are examined stochastically through PDFs. In the homoclinic region, the locally existing chaotic attractor, and coexisting chaotic and periodic attractors are portrayed by the steady-state PDF on the Poincaré section. However, due to the strong attraction of capsizing and the fact that coexisting basins of attraction are bridged by the external noise, no steady-state PDF can be obtained in the heteroclinic region. Thus, in the vicinity of the heteroclinic region with noise present, all roll motion trajectories eventually escape from the bounded motion region to the capsizing region.
3. For small amplitude roll motions, the presence of random noise decreases the orderliness and increases the randomness of the chaotic response. The noise bridges the domains of attraction of coexisting attractors and influences their relative strengths. Moreover, it significantly diminishes the sensitivity of the chaotic roll motion response to initial conditions. Thus noise intensity can be considered as a control parameter, and a small but finite random disturbance could be helpful in identifying the existence of chaotic responses in an experiment.
4. The external noise has an opposite effect in the heteroclinic region. Although for relatively large amplitude roll motions the noise also bridges the domains of attraction of coexisting attractors and scales their relative strengths, the presence of even very weak noise eventually leads to unbounded (capsizing) motions. Thus the 'steady-state' PDF concentrates at plus and minus infinity, which implies that a steady-state chaotic response cannot exist.
5. Heteroclinic chaotic motions and capsize are closely related. The ship can be considered to be in danger of capsize when the response trajectories visit the heteroclinic region. The probability of extreme excursions can be estimated with the time-averaged PDF as an invariant measure. The probability of extreme excursions is elevated with increasing noise intensity, which increases the probability of capsize.

As mentioned in the Introduction, this paper represents a first attempt to study the qualitative behavior of the chaotic motion and capsize of ships in probability space. The goal is to provide a foundation for the stochastic analysis of highly non-linear ocean systems. To keep the analysis manageable and for clarity of presentation, pure roll motion has been assumed. However, it is well-known that for large roll motions, the effect of coupling among roll, heave and sway motions may not be negligible. Thus the conclusions concerning large roll motions obtained in this study should only be interpreted qualitatively. The region of validity of the results will be further examined by using a more complex model of the ship motion and a stochastic description of the wave excitation. In particular, it has been observed that the impact of large breaking waves could be a major cause of capsize.[30] These issues, and potential applications of the probability-space approach, will be addressed in future studies.

ACKNOWLEDGEMENTS

The authors gratefully acknowledge the financial support of the United States Office of Naval Research (Grant No. N00014-92-J-1221). The constructive comments of the reviewers were also appreciated.

REFERENCES

1. Soliman, M. & Thompson, J. M. T., Transition and steady state analysis of capsize phenomena. *Appl. Ocean Res.*, **13** (1991) 82–92.
2. Falzarano, J., Shaw, S. W. & Troesch, A. W., Application of global methods for analyzing dynamical systems to ship rolling motion and capsizing, *Int. J. Bifurcation and Chaos*, **2** (1990) 101–15.
3. Thompson, J. M. T., Chaotic phenomena triggering the escape from a potential well. *Proc. Roy. Soc. London*, **A421** (1989) 195–225.
4. Thompson, J. M. T., Rainey, R. C. T. & Soliman, M. S., Ship stability criteria based on chaotic transition from incursive fractals. *Phil. Trans. Roy. Soc. London*, **332** (1990) 149–67.
5. Virgin, L. N. & Bishop, S. R., Complex dynamics and chaotic responses in the time domain simulations of a floating structure. *Ocean Engng*, **15** (1988) 71–90.
6. Virgin, L. N., Approximate criterion for capsize based on deterministic dynamics. *Dynamics Stability Systems*, **4** (1989) 55–70.
7. Virgin, L. N., A simplified lower-bound criterion for stable rolling motion. *Proc. of the Fourth Int. Conf. on the Stability of Ships and Ocean Vehicles* (STAB'90), Naples, Italy, Vol. 1, 1990, pp. 45–50.
8. Virgin, L. N. & Erickson, B. K., A new approach to the overturning stability of floating structures. *Ocean Engng*, **21** (1994) 67–80.
9. Bulsara, A. R., Schieve, W. C. & Jacobs, E. W., Homoclinic chaos in systems perturbed by weak Langevin noise. *Physical Rev. A*, **41** (1990), 668–81.
10. Frey, M. & Simiu, E., Equivalence between motions with

noise-induced jumps and chaos with Smale horseshoes. *Proc. Ninth Engng Mech. Conf. ASCE*, Texas A&M University, College Station, Texas, 24–27 May 1992, pp. 660–3.
11. Kapitaniak, T., *Chaos in Systems with Noise*. World Scientific, Singapore, 1988.
12. Bulsara, A. R. & Jacobs, E. W., Noise effects in a non-linear dynamic system: the rf superconducting quantum interference device. *Physical Rev. A*, **42** (1990) 4614–21.
13. Kunert, A. & Pfeiffer, F., Description of chaotic motion by an invariant distribution at the example of the driven Duffing oscillator. *Int. Series of Numerical Math.* **97** (1991) 225–30.
14. Kifer, Y., Attractors via random perturbations. *Com. Math. Phys.*, **121** (1989) 445–55.
15. Jung, P. & Hänggi, P., Invariant measure of a driven non-linear oscillator with external noise. *Phys. Rev. Let.*, **65** (1990) 3365–8.
16. Guckenheimer, J. & Holmes, P., *Non-linear Oscillations, Dynamical Systems, and Bifurcations of Vector Fields*. Springer, New York, 1983.
17. Wiggins, S., *Global Bifurcations and Chaos: Analytical Methods*. Springer, New York, 1988.
18. Wiggins, S., *Introduction to Applied Non-linear Dynamical Systems and Chaos*. Springer, New York, 1990.
19. Yim, S. C. S. & Lin, H., Non-linear impact and chaotic response of slender rocking objects. *J. Engng Mech.*, **117** (1991) 2079–100.
20. Graham, R., Path integral solution of general diffusion processes. *Zeitschrift für Physiks B*, **26** (1977) 281–90.
21. Risken, H., *The Fokker–Planck Equation: Methods of Solution and Applications*. Springer, Berlin, 1984.
22. Naess, A. & Johnsen, J. M., Statistics of non-linear dynamic systems by path integrations. *Non-linear Stochastic Mechanics*, IUTAM Symposium, Turin, 1991, pp. 401–9.
23. Stratonovich, R. L., *Topics in the Theory of Random Noise*. Gordon and Breach, 1967.
24. Wehner, M. F. & Wolfer, W. G., Numerical evaluation of path-integral solutions to Fokker–Planck equations. *Phys. Rev. A*, **27** (1983) 2663–70.
25. Shinozuka, M., Simulation of multivariate and multi-dimensional random processes. *J. Acoust. Soc. Am.*, **49** (1971) 357–67.
26. Yim, S. C. S. & Lin, H., Probabilistic analysis of a chaotic dynamical system. *Applied Chaos*, Ch. 9. John Wiley, New York, 1992, pp. 219–41.
27. Ochi, M. K., *Applied Probability and Stochastic Processes*. John Wiley, New York, 1990.
28. Lin, Y. K., *Probabilistic Theory of Structural Dynamics*. McGraw–Hill, 1967.
29. Naess, A. & Johnsen, J. M., Response statistics of non-linear, compliant offshore structures by the path integral solution method. *Probabilistic Engng Mech.*, **8** (1993) 91–106.
30. Myrhaug, D. & Kjeldsen, S. R., Parametric modeling of joint probability density distributions for steepness and asymmetry in deep water waves. *Appl. Ocean Res.*, **6** (1984) 207–26.